

Pre-training Point Cloud Compact Model with Partial-aware Reconstruction

Yaohua Zha^{1,2} Yanzi Wang¹ Tao Dai³* Shu-Tao Xia^{1,2}

¹Tsinghua Shenzhen International Graduate School, Tsinghua University

²Research Center of Artificial Intelligence, Peng Cheng Laboratory

³College of Computer Science and Software Engineering, Shenzhen University

Abstract

The pre-trained point cloud model based on Masked Point Modeling (MPM) has exhibited substantial improvements across various tasks. However, two drawbacks hinder their practical application. Firstly, the positional embedding of masked patches in the decoder results in the leakage of their central coordinates, leading to limited 3D representations. Secondly, the excessive model size of existing MPM methods results in higher demands for devices. To address these, we propose to pre-train **Point** cloud Compact Model with **Partial-aware Reconstruction**, named **Point-CPR**. Specifically, in the decoder, we couple the vanilla masked tokens with their positional embeddings as randomly masked queries and introduce a partial-aware prediction module before each decoder layer to predict them from the unmasked partial. It prevents the decoder from creating a shortcut between the central coordinates of masked patches and their reconstructed coordinates, enhancing the robustness of models. We also devise a compact encoder composed of local aggregation and MLPs, reducing the parameters and computational requirements compared to existing Transformer-based encoders. Extensive experiments demonstrate that our model exhibits strong performance across various tasks, especially surpassing the leading MPM-based model PointGPT-B with only 2% of its parameters. The code will be released.

1 Introduction

3D point cloud perception, as a crucial application of deep learning, has achieved significant success across various areas such as autonomous driving, robotics, and virtual reality. Point cloud self-supervised learning [Xie *et al.*, 2020; Afham *et al.*, 2022; Yu *et al.*, 2022], capable of learning universal representations from extensive unlabeled point cloud data, has gained much attention. Masked point modeling (MPM) [Yu *et al.*, 2022; Pang *et al.*, 2022; Liu *et al.*, 2022; Zha *et al.*, 2024a], as an important self-supervised paradigm,

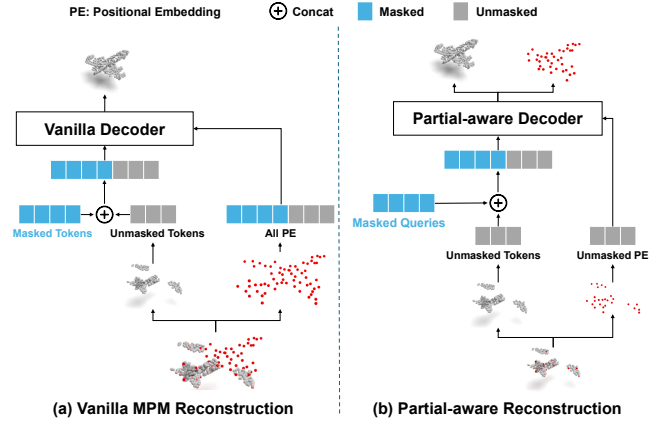


Figure 1: Comparison of (a) vanilla MPM reconstruction and (b) our partial-aware reconstruction. Our reconstruction does not require the center coordinates of masked patches as input. The encoding process is omitted in the figure.

has become mainstream in point cloud analysis and has gained immense success across diverse point cloud tasks.

The classical MPM [Pang *et al.*, 2022] is inspired by masked image modeling (MIM) [Bao *et al.*, 2021; He *et al.*, 2022; Xie *et al.*, 2022] and begins by dividing the point cloud into patches, utilizing the central point coordinate of each patch to denote their positions. The patch content is represented by the relative coordinates of other points concerning the central point. By random masking and reconstruction, it predicts the relative coordinates of the masked patches. Despite the significant success, two drawbacks continue to limit the practical application of these MPM-based models.

The introduction of positional embedding of masked patches in the decoder results in the leakage of the central coordinates, leading to limited 3D representations. In classical MIM [He *et al.*, 2022], the sequence order of each image patch provides positional embedding, while their content, *e.g.* pixels, offers semantic details. Reconstructing the masked patches’ semantic content relies on their positional embedding. However, in most point cloud data, the points are disordered, and only point coordinates are available. Existing MPM methods utilize the absolute coordinates of the central point of each patch to represent its position, while the

*Corresponding author.

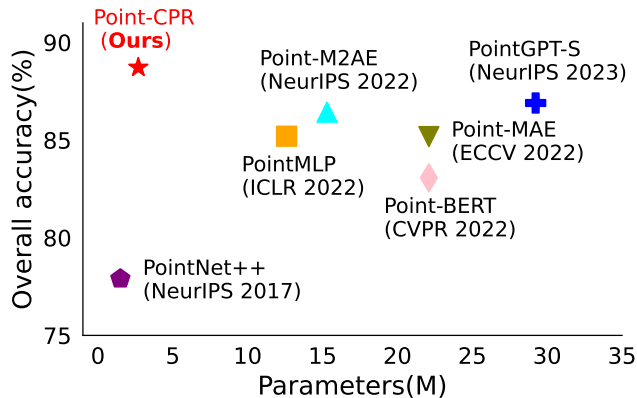


Figure 2: Accuracy-parameters tradeoff on ScanObjectNN. Our Point-CPR performs best. Please refer to Section 4.2 for details.

relative coordinates of the other points in a patch to the central point represent its semantics, leading to a coupling of semantics and position. When reconstructing masked patches, the center point coordinates of masked patches are fed into the decoder as positional embeddings to predict their semantics, *e.g.* relative coordinates. As depicted in Figure 1 (a), the overall contour of the complete point cloud remains available during reconstruction. While this approach does alleviate learning difficulties caused by coordinates autoregression, existing methods that direct transfer from MIM may lead to shortcuts in learning reconstructed semantic coordinates due to the leakage of the central point coordinates of the patch, resulting in limited 3D representations.

Another factor hindering the practical application of these models is their significant demands on both model size and computational complexity, imposing high requirements on practical devices. Indeed, in practical applications of point clouds, models are often deployed on embedded devices such as robots or VR headsets, where strict constraints exist regarding the model’s size and complexity. As shown in Fig 2, PointNet++ [Qi *et al.*, 2017b], the most popular point cloud analysis model, has merely 1.5M parameters for classification. In contrast, MPM methods like Point-MAE [Pang *et al.*, 2022] require 22.1M parameters and complexity exponentially grows with an increase in the number of points. This significant disparity imposes even higher demands on practical devices, particularly when facing limited resources.

To solve the above-mentioned issues, we propose to pre-train **Point** cloud **Compact Model** with **Partial-aware Reconstruction**, named **Point-CPR**. Specifically, unlike the existing approach of embedding each masked patch by combining positional embedding and its’ mask tokens in the decoder, we assigned randomly initialized masked query to represent the combined token of each masked patch. At this point, as shown in Figure 1(b), the central coordinates of each masked patch are unavailable to the decoder. Therefore, we design a partial-aware prediction module before each layer of the decoder to predict tokens of the masked patches from the unmasked partial point cloud. Due to the decoded masked queries coupling the positional and semantic information, we

not only reconstruct the semantic relative coordinates of the masked patches but also reconstruct their center coordinates. This dual reconstruction of semantics and positions disrupts the learning shortcuts caused by positional leakage in existing MPMs, making the pre-training more challenging and conducive to getting robust 3D representation.

To mitigate the high demands of pre-trained models on practical devices, we also devise a compact encoder to replace the vanilla Transformer-based encoder [Vaswani *et al.*, 2017]. Our compact encoder is exclusively composed of lightweight local aggregation modules and residual MLPs, thereby eschewing the computational complexity and continued memory access inherent in Self-Attention mechanisms. By doing so, as depicted in Figure 2, our pre-trained model exhibits a mere 2.7M parameters, significantly smaller than the 22.1M of Point-MAE and 29.2M of PointGPT-S [Chen *et al.*, 2023b]. Furthermore, these reduced parameters mitigate the risk of overfitting in downstream tasks, allowing the model’s performance to surpass existing MPM models.

Our main contributions are summarized as follows:

- We propose a partial-aware reconstruction strategy for point cloud self-supervised learning, mitigating the issue of positional leakage during existing reconstruction caused by the inherent disorder and coordinate-based nature of point clouds.
- We design a compact encoder, that mitigates the high demands of pre-trained models on practical devices and also mitigates the risk of overfitting in downstream tasks.
- Extensive experiments demonstrate that our model exhibits strong performance across various tasks, especially surpassing the leading MPM-based model PointGPT-B with only 2% of its parameters.

2 Related Work

2.1 Point Cloud Self-supervised Pre-training

Point cloud self-supervised pre-training has achieved remarkable improvement in many point cloud tasks. This approach first applies a pretext task to learn the latent 3D representation and then transfers it to various downstream tasks. Point-Contrast [Xie *et al.*, 2020] and CrossPoint [Afham *et al.*, 2022] initially explored utilizing contrastive learning [Oord *et al.*, 2018; Tian *et al.*, 2020] for learning 3D representations, which achieved some success; however, there were still some shortcomings in capturing fine-grained semantic representations. Recently, masked point modeling methods [Yu *et al.*, 2022; Pang *et al.*, 2022; Liu *et al.*, 2022; Chen *et al.*, 2023b; Zha *et al.*, 2024a; Zha *et al.*, 2024b] demonstrated significant improvements in learning fine-grained point cloud representations through masking and reconstruction. However, they still learned limited 3D representations. Many methods [Dong *et al.*, 2022; Guo *et al.*, 2023; Chen *et al.*, 2023a] have attempted to leverage multimodal knowledge to assist MPM in learning more generalized representations, yielding significant improvements but also introducing additional computational pressure. In this paper, we unleash the full potential of single-modal point cloud masking reconstruction

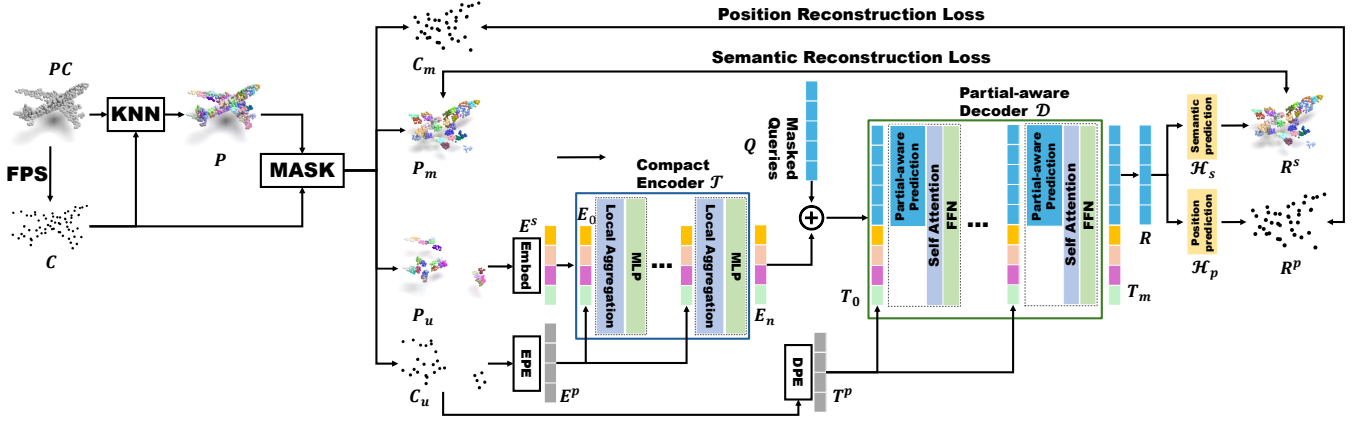


Figure 3: The pipeline of our Point-CPR. Given a point cloud, we first encode unmasked features by our compact encoder. Then, we concatenate random masked queries with the encoded features and feed them into our partial-aware decoder to decode the masked portion. Finally, we perform dual reconstruction of semantic and positional coordinates of masked patches.

by addressing the issue of positional leakage during reconstruction in existing MPMs, enabling the acquisition of more robust 3D representations.

2.2 Deep network architecture for point cloud

Point clouds, as 3D data directly sampled from scanning devices, inherently exhibit irregularity and disorder. To employ deep neural networks for point cloud analysis, various structures have been developed [Qi et al., 2017a; Wang et al., 2019; Zha et al., 2023a; Xiong et al., 2023; Liang et al., 2024; Zhou et al., 2024]. PointNet [Qi et al., 2017a], a pioneer in point cloud analysis, introduced an MLP-based network to address the disorder of point clouds. Subsequently, PointNet++ [Qi et al., 2017b] further proposed adaptive aggregation of multiscale features on MLPs and incorporated local point sets for effective feature learning. DGCNN [Wang et al., 2019] introduced the graph convolutional networks dynamically computing local graph neighboring nodes to extract geometric information. PointMLP [Ma et al., 2022] suggested efficient point cloud representation solely relying on pure residual MLPs. Recently, many Transformer-based models [Guo et al., 2021; Misra et al., 2021; Pang et al., 2022; Wu et al., 2022; Wu et al., 2024], benefiting from attention mechanisms, have achieved notable improvements in point cloud analysis. However, this led to a significant increase in model size, posing considerable challenges for practical applications. In this paper, we focus on designing more compact point cloud network architectures specific to pre-training models.

3 Methodology

The overall pipeline of our Point-CPR is shown in Figure 3, primarily composed of a mask and embedding layer, a compact encoder, and a partial-aware decoder for reconstruction. In this section, we first introduce the overall pre-training pipeline of our Point-CPR (§ 3.1). Next, we provide a detailed exposition of the design of the compact encoder employed for efficient feature extraction (§ 3.2). Finally, we

detail the design of our partial-aware decoder for robust 3D representations (§ 3.3).

3.1 The Pipeline of Point-CPR

Patching, Masking, and Embedding

Given an input point cloud $PC \in \mathbb{R}^{N \times 3}$ with N points, we initially downsample a central point cloud $C \in \mathbb{R}^{M \times 3}$ with M points by farthest point sampling (FPS). Then, we perform K-Nearest Neighborhood (KNN) around C to divide PC into M point patches $P \in \mathbb{R}^{M \times K \times 3}$. Following this, we randomly mask a portion of C and P , resulting in masked elements $C_m \in \mathbb{R}^{(1-r)M \times 3}$ and $P_m \in \mathbb{R}^{(1-r)M \times K \times 3}$, along with unmasked elements $C_u \in \mathbb{R}^{rM \times 3}$ and $P_u \in \mathbb{R}^{rM \times K \times 3}$, where r denotes the unmask ratio. Finally, we use lightweight PointNet [Qi et al., 2017a] and MLP as semantic embedding layer (Embed) and position embedding layer (PE) respectively to extract semantic tokens $E^s \in \mathbb{R}^{rM \times d}$ and central position embedding $E^p \in \mathbb{R}^{rM \times d}$ for the unmasked patches. These embeddings are then added to obtain the initial features $E_0 \in \mathbb{R}^{rM \times d}$, where d is the feature dimension.

Encoder

We employ our compact encoder \mathcal{T} to extract features from the unmasked features E_0 . This encoder consists of a series of n encode layers, each layer incorporating a local aggregation module and an MLP layer, detailed in Figure 4. For the input feature E_{i-1} of the i -th layer, after adding its positional embedding E^p , it feeds to the i -th encoding layer \mathcal{T}_i to obtain the feature E_i . Therefore, the forward process of each encoder layer is defined as:

$$E_i = \mathcal{T}_i(E_{i-1} + E^p), \quad i = 1, \dots, n \quad (1)$$

Decoder

In the decoding stage, unlike previous MPM methods that require fusing masked tokens and positional embeddings to represent the features of masked patches, we use randomly initialized mask queries $Q \in \mathbb{R}^{rM \times d}$ to represent them. Subsequently, we employ our partial-aware decoder \mathcal{D} to decode the masked features. Specifically, we first concatenate

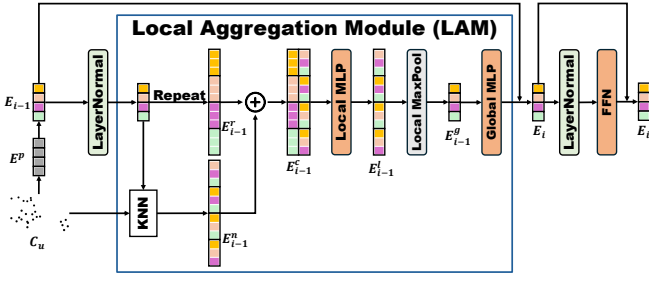


Figure 4: The structure of our compact encoder layer and our compact encoder consists of n stacked compact encoder layers.

the features $E_n \in \mathbb{R}^{rM \times d}$ of the unmasked patches with the randomly initialized mask queries Q to obtain the input $T_0 \in \mathbb{R}^{M \times d}$ for the decoder. Then, we embed the decoder positional embedding $T^p \in \mathbb{R}^{rM \times d}$ of the unmasked patches. Finally, for the input feature T_{i-1} of the i -th decoder layer, we add the unmasked tokens (e.g. the first rM tokens $T_{i-1}[rM:]$) to their positional embeddings T^p and concatenate the results with the next rM masked query tokens $T_{i-1}[rM:]$. Therefore, the forward process of each decoder layer is defined as:

$$T_i = \mathcal{D}_i(\{T_{i-1}[rM:] + T^p; T_{i-1}[rM:] \}_0), i = 1, \dots, m, \quad (2)$$

where $\{ \}_0$ denotes concatenation along the token dimension.

Reconstruction

We utilize the features $R = T_m[rM:]$ decoded by the decoder to perform the 3D reconstruction. In contrast to previous MPM methods that only reconstruct semantics, we reconstruct the masked patch from both semantic and central coordinates. We employ multi-layer MLPs to construct semantic reconstruction head \mathcal{H}_s and central position reconstruction head \mathcal{H}_p and our reconstruction target is to recover the central coordinates $R_p = \mathcal{H}_p(R)$ and relative coordinates $R_s = \mathcal{H}_s(R)$ of the masked patches.

We use the l_2 Chamfer Distance [Fan et al., 2017] (CD) as our reconstruction loss. Therefore, our loss function \mathcal{L} is as follows

$$\mathcal{L} = CD(R^s, P_m) + CD(R^p, C_m) \quad (3)$$

3.2 Compact Encoder

The classical Transformer [Vaswani et al., 2017] relies on the Self-Attention mechanism to perceive long-range correlations among all patches globally and has achieved great success in language and image domains. However, there remains uncertainty about whether directly transferring a Transformer-based encoder is suitable for point cloud data. Firstly, applications of point clouds are more inclined towards practical consumer devices, such as VR glasses and automobiles. The hardware resources of these devices are limited, imposing higher limits on the model size and complexity, and the Transformer-based backbone demands significantly more resources than traditional networks, as illustrated in

Figure 2. Secondly, extensive research [Qi et al., 2017b; Wang et al., 2019; Misra et al., 2021] also indicates that the perception of local geometry in point cloud data far outweighs the need for global perception. Therefore, the computation of long-range correlations in Self-Attention leads to a considerable amount of redundant calculations. To address these practical issues, we propose a compact encoder based on local aggregation.

Our compact encoder consists of n stacked compact encoder layers, each layer comprising a local aggregation module (LAM) and a feed-forward network (FFN), as shown in Figure 4. For the i -th encoder layer, the output (E_{i-1}) of the preceding layer, augmented with the positional embedding and layer normal, is initially fed to the Local Aggregation Module (LAM) for aggregating local geometric. Afterward, the result is added to the input residual, passed through layer normalization, and finally fed into a Feed-forward Network (FFN) to obtain the ultimate output feature (E_i). This process can be formalized as follows:

$$E_i = E_{i-1} + l_i(n_i^1(E_{i-1}), C_u) \quad (4)$$

$$E_i = E_i + f_i(n_i^2(E_i)) \quad (5)$$

where $l(\cdot)$ represents the LAM, $n(\cdot)$ represents layer normalization, and $f(\cdot)$ represents the FFN.

In the Local Aggregation Module, we first use the k-nearest neighbors algorithm based on the features E_{i-1} and its central coordinates C_u to find the k nearest neighbors feature $E_{i-1}^n \in \mathbb{R}^{(1-r)kM \times C}$ for each token in E_{i-1} . We then replicate each token of E_{i-1} k times and concatenate them with their corresponding neighbors to obtain $E_{i-1}^c \in \mathbb{R}^{(1-r)M \times 2C}$. Next, Local MLP performs a non-linear mapping on all local neighboring features to capture local geometric information. Subsequently, local max pooling is applied to aggregate all local features for each patch. Finally, Global MLP maps all patches to obtain locally enhanced features $E_i \in \mathbb{R}^{(1-r)M \times C}$. Our LAM consists of only two simple MLP layers, significantly reducing computational requirements compared to redundant Self-Attention mechanisms. Additionally, further experimental analysis indicates that our compact encoder, due to a significant reduction in parameters, can effectively alleviate the overfitting issues associated with Transformers in downstream tasks. Please refer to supplementary files for details.

3.3 Partial-aware Decoder

To address the issue of limited representation caused by the position leakage of the center coordinates of invisible patches during point cloud reconstruction in vanilla MPM, we propose predicting the features of these invisible patches without relying on their center points as input. We introduce a partial-aware decoder to simultaneously reconstruct the center coordinates and semantic coordinates of invisible patches. Its structure is depicted in Figure 3, consisting of m stacked decoding layers. Each layer is composed of a partial-aware prediction module and a standard Transformer layer. We do not replace the original Transformer structure in the decoder, as the decoder is discarded during downstream fine-tuning.

Method	Reference	Pre-training	#Params (M)	GFLOPs	ScanObjectNN			ModelNet40	
					OBJ-BG	OBJ-ONLY	PB-T50-RS	w/o Vote	w/ Vote
<i>Supervised Learning Only</i>									
PointNe [Qi et al., 2017a]	CVPR 2017	✗	3.5	0.5	73.3	79.2	68	89.2	-
PointNet++ [Qi et al., 2017b]	NeurIPS 2017	✗	1.5	1.7	82.3	84.3	77.9	90.7	-
DGCNN [Wang et al., 2019]	TOG 2019	✗	1.8	2.4	82.8	86.2	78.1	92.9	-
MVTN [Hamdi et al., 2021]	ICCV 2021	✗	11.2	43.7	92.6	92.3	82.8	93.8	-
PointMLP [Ma et al., 2022]	ICLR 2022	✗	12.6	31.4	-	-	85.2	94.1	94.5
P2P-HorNet [Wang et al., 2022]	NeurIPS 2022	✗	195.8	34.6	-	-	89.3	94.0	-
<i>Single Modal Self-Supervised Learning</i>									
STRL [Huang et al., 2021]	ICCV 2021	CL	-	-	-	-	-	93.1	-
Point-BERT [Yu et al., 2022]	CVPR 2022	MPM	22.1	4.8	87.43	88.12	83.07	92.7	93.2
Point-MAE [Pang et al., 2022]	ECCV 2022	MPM	22.1	4.8	90.02	88.29	85.18	93.2	93.8
Point-M2AE [Zhang et al., 2022a]	NeurIPS 2022	MPM	15.3	3.6	91.22	88.81	86.43	93.4	94.0
PointGPT-S [Chen et al., 2023b]	NeurIPS 2023	MPM	29.2	4.5	91.63	90.02	86.88	-	94.0
PointGPT-B [Chen et al., 2023b]	NeurIPS 2023	MPM	120.5	36.2	93.60	92.50	89.60	-	94.2
IDPT [Zha et al., 2023b]	ICCV 2023	MPM	23.5	-	93.63	93.12	88.51	93.3	94.4
PointFEMAE [Zha et al., 2024a]	AAAI 2024	MPM	27.4	-	95.18	93.29	90.22	94.0	94.5
Point-CPR	-	MPM	2.7	1.9	93.80	93.46	88.72	93.6	94.1
<i>Multimodal Self-Supervised Learning</i>									
ACT [Dong et al., 2022]	ICLR 2023	MMPM	22.1	4.8	93.29	91.91	88.21	93.2	93.7
I2P-MAE [Zhang et al., 2022b]	CVPR 2023	MMPM	15.3	3.6	94.15	91.57	90.11	93.7	94.1
TAP+PointMLP [Wang et al., 2023]	ICCV 2023	MMPM	12.6	31.4	-	-	88.50	94.0	-
Recon [Qi et al., 2023]	ICML 2023	MMPM	44.3	5.3	95.18	93.29	90.63	94.1	94.5

Table 1: Classification accuracy on real-scanned (ScanObjectNN) and synthetic (ModelNet40) point clouds. In ScanObjectNN, we report the overall accuracy (%) on three variants. In ModelNet40, we report the overall accuracy (%) for both without and with voting. ”#Params” represents the model’s parameters and GFLOPs refer to the model’s floating point operations. CL, MPM, and MMPM respectively refer to pre-training strategies based on contrastive learning, single-modal masked point modeling, and multimodal masked point modeling.

We rely on the partial-aware prediction module to predict the feature of invisible patches, and its structure is illustrated in Figure 5. For the i -th decoding layer, we first split the output T_{i-1} of the previous layer into masked query features Q_{i-1} representing invisible patches and features K_{i-1} representing visible patches. For the visible K_{i-1} , we add position embedding T^p to it. Then, we apply layer normalization separately to Q_{i-1} and K_{i-1} . Afterward, we apply self-attention to Q_{i-1} , followed by adding the forward residual, to capture semantics across all query scales. Since Q_{i-1} represents all invisible patches, predicting the semantics of the invisible patches from the visible portion is crucial. Cross-attention, as a classical technique for capturing cross-domain semantic correlations, can effectively perceive the geometry of point clouds from visible regions and transfer this information to invisible queries. Therefore, we further employ cross-attention to predict invisible queries from visible patch tokens. Specifically, we perform cross-attention by using the Q_{i-1} as the query, and K'_{i-1} as both key and value. Afterward, we use FFN for non-linear mapping to obtain a query Q'_{i-1} that perceives the visible point cloud. Finally, we concatenate Q'_{i-1} and K'_{i-1} along the patch dimension to obtain the output of the Partial-aware Prediction Module (PPM), denoted as T_i . We feed it into a standard Transformer layer for further decoding, as illustrated in Figure 3.

4 Experiments

4.1 Pre-training on ShapeNet

For a fair comparison, we use ShapeNet [Chang et al., 2015] as our pre-training dataset, encompassing over 50,000 distinct

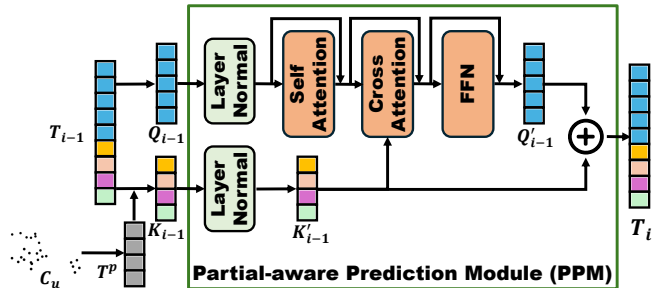


Figure 5: The structure of our partial-aware prediction module.

3D models spanning 55 prevalent object categories. We extract 1024 points from each 3D model to serve as input for pre-training. The input point cloud is further divided into 64 point patches, with each patch containing 32 points.

4.2 Fine-tuning on Downstream Tasks

We assess the performance of our pre-trained model by fine-tuning our models on various downstream tasks, including object classification, scene-level detection, part segmentation, and low-level completion tasks.

Object Classification

We initially assess the overall classification accuracy of our pre-trained models on both real-scanned (ScanObjectNN [Uy et al., 2019]) and synthetic (ModelNet40 [Wu et al., 2015]) datasets. ScanObjectNN is a prevalent dataset consisting of approximately 15,000 real-world scanned point cloud samples from 15 categories. These objects represent indoor

scenes and are often characterized by cluttered backgrounds and occlusions caused by other objects. ModelNet40 is a well-known synthetic point cloud dataset, comprising 12,311 meticulously crafted 3D CAD models distributed across 40 categories. We follow the practices of previous studies [Dong et al., 2022; Qi et al., 2023; Zhang et al., 2022b]. For the ModelNet40 dataset, we sample 1024 points for each instance and report both the overall accuracy without voting and with voting. For the ScanObjectNN dataset, we sample 2048 points for each instance, employ data augmentation of simple rotations and report results without voting mechanisms.

As presented in Table 1, firstly, compared to recent MPM-based approaches, our Point-CPR achieves state-of-the-art performance in most datasets. Notably, our method demands minimal computational resources, *e.g.* 2.7M parameters and 1.9 GFLOPs, which is significantly lower than other methods. Specifically, compared to the leading MPM approach, PointGPT-B [Chen et al., 2023b], our method utilizes only 2.2% of its parameter count. The results of PointGPT-B are derived from the official repository and indicate the outcomes without post-pre-training. Secondly, our method surpasses the majority of multimodal MPM-based approaches (MMPM), ranking just below the leading Recon. This is still highly competitive as Recon [Qi et al., 2023] benefits from the supplementary knowledge of image, and language modalities, while also requiring significantly more parameters than our method.

Object Detection

We further assess the object detection performance of our pre-trained model on the more challenging scene-level point cloud dataset, ScanNet [Dai et al., 2017], to evaluate our model’s scene understanding capabilities. Following the previous pre-trained model [Liu et al., 2022; Dong et al., 2022], we use 3DETR [Misra et al., 2021] as the baseline and only replace the Transformer-based encoder of 3DETR with our pre-trained compact encoder. Subsequently, the entire model is fine-tuned for object detection. In contrast to previous approaches [Liu et al., 2022; Dong et al., 2022; Chen et al., 2023a], which necessitate pre-train on large-scale scene-level point clouds like ScanNet, our approach directly utilizes models pre-trained on ShapeNet. This further emphasizes the generalizability of our pre-trained models to both object-level point clouds and scene-level point clouds.

Table 2 showcases our experimental findings, indicating a 6.6% improvement on AP_{50} over the previous leading MPM method, ACT [Dong et al., 2022]. This demonstrates a notable superiority of our approach over prior contrastive learning-based and MPM-based methods. This superiority derives from two key aspects: firstly, our proposed compact encoder, owing to its more condensed local structural perception capability, notably surpasses existing Transformer-based encoders in scene analysis. Secondly, our introduced pre-trained model with partial-aware reconstruction also provides superior prior for object detection tasks.

Part Segmentation

We also assess the performance of Point-CPR in part segmentation using the ShapeNetPart dataset [Chang et al., 2015], comprising 16,881 samples across 16 categories. We utilize

Methods	Pre-training	AP_{25}	AP_{50}
VoteNet [Qi et al., 2019](baseline)	✗	58.6	33.5
PointContrast [Xie et al., 2020]	CL	58.5	38.0
STRL [Huang et al., 2021]	CL	-	38.4
DepthContrast [Zhang et al., 2021]	CL	64.0	42.9
3DETR [Misra et al., 2021](baseline)	✗	62.1	37.9
Point-BERT [Yu et al., 2022]	MPM	61.0	38.3
MaskPoint [Liu et al., 2022]	MPM	63.4	40.6
PiMAE [Chen et al., 2023a]	MMPM	62.6	39.4
TAP [Wang et al., 2023]	MMPM	63.0	41.4
ACT [Dong et al., 2022]	MMPM	63.8	42.1
Point-CPR	MPM	64.1	48.7

Table 2: Object detection results on ScanNet. We adopt the average precision with 3D IoU thresholds of 0.25 (AP_{25}) and 0.5 (AP_{50}) for the evaluation metrics.

the same segmentation head after the pre-trained encoder as in previous works [Pang et al., 2022; Zhang et al., 2022a] for fair comparison. The head only conducts simple upsampling for point tokens at different stages and concatenates them alone with the feature dimension as the output. As shown in Table 3, our Point-CPR exhibits competitive performance among both existing CL-based and MPM-based methods and is slightly inferior to 2 MMPM-based methods. These results demonstrate that our approach exhibits superior performance in tasks such as part segmentation, which demands a more fine-grained understanding of point clouds.

Point Cloud Completion

The previous pre-trained models required the centroid coordinates of the masked patches to serve as positional priors during the reconstruction, hence these models couldn’t be directly applied to real point cloud reconstruction tasks. Our pre-trained model benefits from the proposed partial-aware reconstruction mechanism, enabling our decoder entirely independent of any unknown point cloud priors. Consequently, it can be directly applied to low-level reconstruction tasks, such as point cloud completion. Therefore, we first evaluate the performance of our pre-trained model on the task of point cloud completion and compare it with the state-of-the-art point cloud completion methods.

We evaluate the transferability of our pre-trained model to low-level tasks by fine-tuning it on the classic point cloud completion dataset, PCN [Yuan et al., 2018]. The PCN dataset is created from the ShapeNet dataset, including eight categories with a total of 30974 CAD models. We followed the data processing methods established in previous works [Yu et al., 2021; Li et al., 2023] and used the l_1 Chamfer Distance [Fan et al., 2017] to evaluate the results. As shown in Table 4, our approach exhibits substantial improvements in aircraft, cabinet, and car completion compared to the previous leading method ProxyFormer [Li et al., 2023] and achieves the lowest average Chamfer Distance, highlighting the significant advantage of our partial-aware reconstruction for point cloud pre-training.

Methods	Pre-training	mIoU _c	mIoU _I
<i>Supervised Learning Only</i>			
PointNet [Qi et al., 2017a]	✗	80.4	83.7
PointNet++ [Qi et al., 2017b]	✗	81.9	85.1
DGCNN [Wang et al., 2019]	✗	82.3	85.2
PointMLP [Ma et al., 2022]	✗	84.6	86.1
<i>Single-Modal Self-Supervised Learning</i>			
Transformer [Vaswani et al., 2017]	MPM	83.4	84.7
Transformer-OcCo [Wang et al., 2021]	CL	83.4	85.1
PointContrast [Xie et al., 2020]	CL	-	85.1
CrossPoint [Afham et al., 2022]	CL	-	85.5
IDPT [Zha et al., 2023b]	MPM	83.8	85.9
Point-BERT [Yu et al., 2022]	MPM	84.1	85.6
MaskPoint [Liu et al., 2022]	MPM	84.4	86.0
Point-MAE [Pang et al., 2022]	MPM	84.2	86.1
PointGPT-S [Chen et al., 2023b]	MPM	84.1	86.2
PointGPT-B [Chen et al., 2023b]	MPM	84.5	86.4
PointFEMAE [Zha et al., 2024a]	MPM	84.9	86.3
Point-M2AE [Zhang et al., 2022a]	MPM	84.9	86.5
Point-CPR	MPM	85.1	86.5
<i>Multimodal Self-Supervised Learning</i>			
ACT [Dong et al., 2022]	MMPM	84.7	86.1
Joint-MAE [Guo et al., 2023]	MMPM	85.4	86.3
Recon [Qi et al., 2023]	MMPM	84.8	86.4
I2P-MAE [Zhang et al., 2022b]	MMPM	85.2	86.8
TAP+PointMLP [Wang et al., 2023]	MMPM	85.2	86.9

Table 3: Part segmentation results on the ShapeNetPart. The mean IoU across all categories, i.e., mIoU_c (%), and the mean IoU across all instances, i.e., mIoU_I (%) are reported.

Methods	Chamfer Distance (10^{-3}) (↓)								
	Ave	Air.	Cab.	Car	Cha.	Lam.	Sof.	Tab.	Ves.
FoldingNet [Yang et al., 2018]	14.31	9.49	15.80	12.61	15.55	16.41	15.97	13.65	14.99
AtlasNet [Groueix et al., 2018]	10.85	6.37	11.94	10.10	12.06	12.37	12.99	10.33	10.61
PCN [Yuan et al., 2018]	9.64	5.50	22.70	10.63	8.70	11.00	11.34	11.68	8.59
CRN [Wang et al., 2020]	8.51	4.79	9.97	8.31	9.49	8.94	10.69	7.81	8.05
PMP-Net [Wen et al., 2021]	8.73	5.65	11.24	9.64	9.51	6.95	10.83	8.72	7.25
PointTr [Yu et al., 2021]	8.38	4.75	10.47	8.68	9.39	7.75	10.93	7.78	7.29
SnowflakeNet [Xiang et al., 2021]	7.21	4.29	9.16	8.08	7.89	6.07	9.23	6.55	6.40
ProxyFormer [Li et al., 2023]	6.77	4.01	9.01	7.88	7.11	5.35	8.77	6.03	5.98
Point-CPR (Ours)	6.75	3.75	8.81	7.46	7.35	5.71	8.69	6.27	5.98

Table 4: Quantitative comparison of point cloud completion task on PCN. Point resolutions for the output and GT are 16384. For Chamfer Distance, lower is better.

4.3 Ablation Study

Effects of Position Leakage in Decoder

To illustrate the issue of position leakage in the decoding phase of the previous MPM method, we conducted four sets of experiments using the compact encoder settings in classification and detection tasks. A corresponds to training from scratch, B uses the vanilla MPM strategy but does not include position encoding for masked patches in the decoder, C employs the vanilla MPM strategy, and D represents our partial-aware reconstruction strategy.

As shown in Figure 5, comparing A with B, C, and D reveals that the pre-training strategy indeed enhances representational capacity. The comparison between B and C indicates the crucial role of position embedding for masked patches in vanilla MPM pre-training, as it simplifies the reconstruction task, allowing the decoder to learn shortcuts between the center coordinates of masked patches and the relative coordinates of masked patches. However, this also further limits the potential for representation learning. Comparing C and

Index	Pre-training	ScanObjectNN Classification		ScanNetV2 Detection	
		OBJ-ONLY	PB-T50-RS	AP_{25}	AP_{50}
A	✗	90.71	87.47	63.8	46.4
B	Vanilla MPM w/o pos	91.22(↑ 0.51)	87.86(↑ 0.39)	63.6(↓ 0.2)	47.0(↑ 0.6)
C	Vanilla MPM	92.43(↑ 1.72)	88.13(↑ 0.66)	63.9(↑ 0.1)	47.3(↑ 0.9)
D	Partial-aware (Ours)	93.46(↑ 2.75)	88.72(↑ 1.25)	64.1(↑ 0.3)	48.7(↑ 2.3)

Table 5: Comparison of the impact of partial-aware reconstruction strategy and vanilla MPM reconstruction strategy on classification and detection tasks.

D, our method does not use the center coordinates of masked patches as input, making the reconstruction task more challenging, but our partial-aware reconstruction mechanism can learn the unknown from the known, further unleashing the potential for representation learning. The comparison between B and D further illustrates that under the same decoder input, our partial-aware reconstruction greatly unleashes the potential for representation learning. These results strongly demonstrate the effectiveness of our proposed partial-aware reconstruction.

Effects of Compact Encoder

Encoder	ScanObjectNN Classification		ScanNetV2 Detection	
	# Params.(M)	Overall Acc.	AP_{25}	AP_{50}
Transformer	22.1	86.92	60.5	40.6
Compact (Ours)	2.7(↓ 19.4)	87.47(↑ 0.55)	63.8(↑ 3.3)	46.4(↑ 5.8)

Table 6: Effects of Different Encoder. We compare the performance of the Transformer-based encoder and our compact encoder on classification and detection tasks, all experiments are training from scratch.

We explore the performance of our compact encoder by comparing it with a Transformer-based encoder in classification and detection tasks. Table 6 illustrates the classification performance on the real scanned point cloud dataset ScanObjectNN and the detection performance on the ScanNetV2 dataset for two different networks without any pre-training. Our compact encoder outperforms the Transformer-based structure significantly, particularly in detection tasks, with an improvement of up to 5.8% in the AP_{50} metric.

This substantial enhancement is attributed to the compact encoder’s focus on local neighborhood information, crucial for point cloud analysis, especially in large-scale scene-level point clouds. Another contributing factor is the utilization of fewer network parameters; for instance, in classification, we only require 2.7M parameters compared to the Transformer-based model’s 22.1M, which better mitigates network overfitting in existing limited-size point cloud datasets. We provide a detailed explanation of this overfitting phenomenon in the supplementary material. Please refer to the supplementary material for more details.

5 Conclusion

In this paper, we propose Point-CPR, a masking point modeling pre-training framework to solve the limitations of the existing MPM-based methods in practical applications. We first propose partial-aware reconstruction, replacing existing position-embedded masked tokens with random masked

queries and leveraging a partial-aware predict module in the decoder to predict it. This process resolves the limited 3D representations resulting from position leakage of masked patches in previous methods. Secondly, we introduce a compact encoder composed solely of local aggregations and MLPs, replacing the previous Transformer-based encoder to mitigate demands on practical device resources caused by oversized models. Finally, extensive experiments validate the superiority of our proposed approach in both efficiency and performance.

References

- [Afham *et al.*, 2022] Mohamed Afham, Isuru Dissanayake, Dinithi Dissanayake, Amaya Dharmasiri, Kanchana Thilakarathna, and Ranga Rodrigo. Crosspoint: Self-supervised cross-modal contrastive learning for 3d point cloud understanding. In *Proceedings of the IEEE/CVF Conference on Computer Vision and Pattern Recognition*, pages 9902–9912, 2022. 1, 2, 7
- [Bao *et al.*, 2021] Hangbo Bao, Li Dong, Songhao Piao, and Furu Wei. Beit: Bert pre-training of image transformers. *arXiv preprint arXiv:2106.08254*, 2021. 1
- [Chang *et al.*, 2015] Angel X Chang, Thomas Funkhouser, Leonidas Guibas, Pat Hanrahan, Qixing Huang, Zimo Li, Silvio Savarese, Manolis Savva, Shuran Song, Hao Su, et al. Shapenet: An information-rich 3d model repository. *arXiv preprint arXiv:1512.03012*, 2015. 5, 6
- [Chen *et al.*, 2023a] Anthony Chen, Kevin Zhang, Renrui Zhang, Zihan Wang, Yuheng Lu, Yandong Guo, and Shanghang Zhang. Pimae: Point cloud and image interactive masked autoencoders for 3d object detection. In *Proceedings of the IEEE/CVF Conference on Computer Vision and Pattern Recognition*, pages 5291–5301, 2023. 2, 6
- [Chen *et al.*, 2023b] Guangyan Chen, Meiling Wang, Yi Yang, Kai Yu, Li Yuan, and Yufeng Yue. Pointgpt: Auto-regressively generative pre-training from point clouds. *arXiv preprint arXiv:2305.11487*, 2023. 2, 5, 6, 7
- [Dai *et al.*, 2017] Angela Dai, Angel X Chang, Manolis Savva, Maciej Halber, Thomas Funkhouser, and Matthias Nießner. Scannet: Richly-annotated 3d reconstructions of indoor scenes. In *Proceedings of the IEEE conference on computer vision and pattern recognition*, pages 5828–5839, 2017. 6
- [Dong *et al.*, 2022] Runpei Dong, Zekun Qi, Linfeng Zhang, Junbo Zhang, Jianjian Sun, Zheng Ge, Li Yi, and Kaisheng Ma. Autoencoders as cross-modal teachers: Can pre-trained 2d image transformers help 3d representation learning? *arXiv preprint arXiv:2212.08320*, 2022. 2, 5, 6, 7
- [Fan *et al.*, 2017] Haoqiang Fan, Hao Su, and Leonidas J Guibas. A point set generation network for 3d object reconstruction from a single image. In *Proceedings of the IEEE conference on computer vision and pattern recognition*, pages 605–613, 2017. 4, 6
- [Groueix *et al.*, 2018] Thibault Groueix, Matthew Fisher, Vladimir G Kim, Bryan C Russell, and Mathieu Aubry. A papier-mâché approach to learning 3d surface generation. In *Proceedings of the IEEE conference on computer vision and pattern recognition*, pages 216–224, 2018. 7
- [Guo *et al.*, 2021] Meng-Hao Guo, Jun-Xiong Cai, Zheng-Ning Liu, Tai-Jiang Mu, Ralph R Martin, and Shi-Min Hu. Pct: Point cloud transformer. *Computational Visual Media*, 7(2):187–199, 2021. 3
- [Guo *et al.*, 2023] Ziyu Guo, Xianzhi Li, and Pheng Ann Heng. Joint-mae: 2d-3d joint masked autoencoders for 3d point cloud pre-training. *arXiv preprint arXiv:2302.14007*, 2023. 2, 7
- [Hamdi *et al.*, 2021] Abdullah Hamdi, Silvio Giancola, and Bernard Ghanem. MVTN: multi-view transformation network for 3d shape recognition. pages 1–11. IEEE, 2021. 5
- [He *et al.*, 2022] Kaiming He, Xinlei Chen, Saining Xie, Yanghao Li, Piotr Dollár, and Ross Girshick. Masked autoencoders are scalable vision learners. In *Proceedings of the IEEE/CVF Conference on Computer Vision and Pattern Recognition*, pages 16000–16009, 2022. 1
- [Huang *et al.*, 2021] Siyuan Huang, Yichen Xie, Song-Chun Zhu, and Yixin Zhu. Spatio-temporal self-supervised representation learning for 3d point clouds. In *Proceedings of the IEEE/CVF International Conference on Computer Vision*, pages 6535–6545, 2021. 5, 6
- [Li *et al.*, 2023] Shanshan Li, Pan Gao, Xiaoyang Tan, and Mingqiang Wei. Proxyformer: Proxy alignment assisted point cloud completion with missing part sensitive transformer. In *Proceedings of the IEEE/CVF Conference on Computer Vision and Pattern Recognition*, pages 9466–9475, 2023. 6, 7
- [Liang *et al.*, 2024] Dingkan Liang, Xin Zhou, Xinyu Wang, Xingkui Zhu, Wei Xu, Zhikang Zou, Xiaoqing Ye, and Xiang Bai. Pointmamba: A simple state space model for point cloud analysis. *arXiv preprint arXiv:2402.10739*, 2024. 3
- [Liu *et al.*, 2022] Haotian Liu, Mu Cai, and Yong Jae Lee. Masked discrimination for self-supervised learning on point clouds. In *Computer Vision—ECCV 2022: 17th European Conference, Tel Aviv, Israel, October 23–27, 2022, Proceedings, Part II*, pages 657–675. Springer, 2022. 1, 2, 6, 7
- [Ma *et al.*, 2022] Xu Ma, Can Qin, Haoxuan You, Haoxi Ran, and Yun Fu. Rethinking network design and local geometry in point cloud: A simple residual mlp framework. *arXiv preprint arXiv:2202.07123*, 2022. 3, 5, 7
- [Misra *et al.*, 2021] Ishan Misra, Rohit Girdhar, and Armand Joulin. An end-to-end transformer model for 3d object detection. In *Proceedings of the IEEE/CVF International Conference on Computer Vision*, pages 2906–2917, 2021. 3, 4, 6
- [Oord *et al.*, 2018] Aaron van den Oord, Yazhe Li, and Oriol Vinyals. Representation learning with contrastive predictive coding. *arXiv preprint arXiv:1807.03748*, 2018. 2

- [Pang *et al.*, 2022] Yatian Pang, Wenxiao Wang, Francis EH Tay, Wei Liu, Yonghong Tian, and Li Yuan. Masked autoencoders for point cloud self-supervised learning. *arXiv preprint arXiv:2203.06604*, 2022. 1, 2, 3, 5, 6, 7
- [Qi *et al.*, 2017a] Charles R Qi, Hao Su, Kaichun Mo, and Leonidas J Guibas. Pointnet: Deep learning on point sets for 3d classification and segmentation. In *Proceedings of the IEEE conference on computer vision and pattern recognition*, pages 652–660, 2017. 3, 5, 7
- [Qi *et al.*, 2017b] Charles Ruizhongtai Qi, Li Yi, Hao Su, and Leonidas J Guibas. Pointnet++: Deep hierarchical feature learning on point sets in a metric space. *Advances in neural information processing systems*, 30, 2017. 2, 3, 4, 5, 7
- [Qi *et al.*, 2019] Charles R Qi, Or Litany, Kaiming He, and Leonidas J Guibas. Deep hough voting for 3d object detection in point clouds. In *proceedings of the IEEE/CVF International Conference on Computer Vision*, pages 9277–9286, 2019. 6
- [Qi *et al.*, 2023] Zekun Qi, Runpei Dong, Guofan Fan, Zheng Ge, Xiangyu Zhang, Kaisheng Ma, and Li Yi. Contrast with reconstruct: Contrastive 3d representation learning guided by generative pretraining. *arXiv preprint arXiv:2302.02318*, 2023. 5, 6, 7
- [Tian *et al.*, 2020] Yonglong Tian, Dilip Krishnan, and Phillip Isola. Contrastive multiview coding. In *Computer Vision—ECCV 2020: 16th European Conference, Glasgow, UK, August 23–28, 2020, Proceedings, Part XI 16*, pages 776–794. Springer, 2020. 2
- [Uy *et al.*, 2019] Mikaela Angelina Uy, Quang-Hieu Pham, Binh-Son Hua, Thanh Nguyen, and Sai-Kit Yeung. Revisiting point cloud classification: A new benchmark dataset and classification model on real-world data. In *Proceedings of the IEEE/CVF international conference on computer vision*, pages 1588–1597, 2019. 5
- [Vaswani *et al.*, 2017] Ashish Vaswani, Noam Shazeer, Niki Parmar, Jakob Uszkoreit, Llion Jones, Aidan N Gomez, Łukasz Kaiser, and Illia Polosukhin. Attention is all you need. *Advances in neural information processing systems*, 30, 2017. 2, 4, 7
- [Wang *et al.*, 2019] Yue Wang, Yongbin Sun, Ziwei Liu, Sanjay E Sarma, Michael M Bronstein, and Justin M Solomon. Dynamic graph cnn for learning on point clouds. *Acm Transactions On Graphics (tog)*, 38(5):1–12, 2019. 3, 4, 5, 7
- [Wang *et al.*, 2020] Xiaogang Wang, Marcelo H Ang Jr, and Gim Hee Lee. Cascaded refinement network for point cloud completion. In *Proceedings of the IEEE/CVF conference on computer vision and pattern recognition*, pages 790–799, 2020. 7
- [Wang *et al.*, 2021] Hanchen Wang, Qi Liu, Xiangyu Yue, Joan Lasenby, and Matt J Kusner. Unsupervised point cloud pre-training via occlusion completion. In *Proceedings of the IEEE/CVF international conference on computer vision*, pages 9782–9792, 2021. 7
- [Wang *et al.*, 2022] Ziyi Wang, Xumin Yu, Yongming Rao, Jie Zhou, and Jiwen Lu. P2p: Tuning pre-trained image models for point cloud analysis with point-to-pixel prompting. *arXiv preprint arXiv:2208.02812*, 2022. 5
- [Wang *et al.*, 2023] Ziyi Wang, Xumin Yu, Yongming Rao, Jie Zhou, and Jiwen Lu. Take-a-photo: 3d-to-2d generative pre-training of point cloud models. In *Proceedings of the IEEE/CVF International Conference on Computer Vision*, pages 5640–5650, 2023. 5, 6, 7
- [Wen *et al.*, 2021] Xin Wen, Peng Xiang, Zhizhong Han, Yan-Pei Cao, Pengfei Wan, Wen Zheng, and Yu-Shen Liu. Pmp-net: Point cloud completion by learning multi-step point moving paths. In *Proceedings of the IEEE/CVF conference on computer vision and pattern recognition*, pages 7443–7452, 2021. 7
- [Wu *et al.*, 2015] Zhirong Wu, Shuran Song, Aditya Khosla, Fisher Yu, Linguang Zhang, Xiaoou Tang, and Jianxiong Xiao. 3d shapenets: A deep representation for volumetric shapes. In *Proceedings of the IEEE conference on computer vision and pattern recognition*, pages 1912–1920, 2015. 5
- [Wu *et al.*, 2022] Xiaoyang Wu, Yixing Lao, Li Jiang, Xihui Liu, and Hengshuang Zhao. Point transformer v2: Grouped vector attention and partition-based pooling. *Advances in Neural Information Processing Systems*, 35:33330–33342, 2022. 3
- [Wu *et al.*, 2024] Xiaoyang Wu, Li Jiang, Peng-Shuai Wang, Zhijian Liu, Xihui Liu, Yu Qiao, Wanli Ouyang, Tong He, and Hengshuang Zhao. Point transformer v3: Simpler faster stronger. In *Proceedings of the IEEE/CVF Conference on Computer Vision and Pattern Recognition*, pages 4840–4851, 2024. 3
- [Xiang *et al.*, 2021] Peng Xiang, Xin Wen, Yu-Shen Liu, Yan-Pei Cao, Pengfei Wan, Wen Zheng, and Zhizhong Han. Snowflakenet: Point cloud completion by snowflake point deconvolution with skip-transformer. In *Proceedings of the IEEE/CVF international conference on computer vision*, pages 5499–5509, 2021. 7
- [Xie *et al.*, 2020] Saining Xie, Jiatao Gu, Demi Guo, Charles R Qi, Leonidas Guibas, and Or Litany. Point-contrast: Unsupervised pre-training for 3d point cloud understanding. In *European conference on computer vision*, pages 574–591. Springer, 2020. 1, 2, 6, 7
- [Xie *et al.*, 2022] Zhenda Xie, Zheng Zhang, Yue Cao, Yutong Lin, Jianmin Bao, Zhuliang Yao, Qi Dai, and Han Hu. Simmim: A simple framework for masked image modeling. In *Proceedings of the IEEE/CVF Conference on Computer Vision and Pattern Recognition*, pages 9653–9663, 2022. 1
- [Xiong *et al.*, 2023] Jianyu Xiong, Tao Dai, Yaohua Zha, Xin Wang, and Shu-Tao Xia. Semantic preserving learning for task-oriented point cloud downsampling. In *ICASSP 2023-2023 IEEE International Conference on Acoustics, Speech and Signal Processing (ICASSP)*, pages 1–5. IEEE, 2023. 3

- [Yang *et al.*, 2018] Yaoqing Yang, Chen Feng, Yiru Shen, and Dong Tian. Foldingnet: Point cloud auto-encoder via deep grid deformation. In *Proceedings of the IEEE conference on computer vision and pattern recognition*, pages 206–215, 2018. 7
- [Yu *et al.*, 2021] Xumin Yu, Yongming Rao, Ziyi Wang, Zuyan Liu, Jiwen Lu, and Jie Zhou. PointR: Diverse point cloud completion with geometry-aware transformers. In *Proceedings of the IEEE/CVF international conference on computer vision*, pages 12498–12507, 2021. 6, 7
- [Yu *et al.*, 2022] Xumin Yu, Lulu Tang, Yongming Rao, Tiejun Huang, Jie Zhou, and Jiwen Lu. Point-bert: Pre-training 3d point cloud transformers with masked point modeling. In *Proceedings of the IEEE/CVF Conference on Computer Vision and Pattern Recognition*, pages 19313–19322, 2022. 1, 2, 5, 6, 7
- [Yuan *et al.*, 2018] Wentao Yuan, Tejas Khot, David Held, Christoph Mertz, and Martial Hebert. Pcn: Point completion network. In *2018 international conference on 3D vision (3DV)*, pages 728–737. IEEE, 2018. 6, 7
- [Zha *et al.*, 2023a] Yaohua Zha, Rongsheng Li, Tao Dai, Jianyu Xiong, Xin Wang, and Shu-Tao Xia. Sfr: Semantic-aware feature rendering of point cloud. In *ICASSP 2023-2023 IEEE International Conference on Acoustics, Speech and Signal Processing (ICASSP)*, pages 1–5. IEEE, 2023. 3
- [Zha *et al.*, 2023b] Yaohua Zha, Jinpeng Wang, Tao Dai, Bin Chen, Zhi Wang, and Shu-Tao Xia. Instance-aware dynamic prompt tuning for pre-trained point cloud models. *arXiv preprint arXiv:2304.07221*, 2023. 5, 7
- [Zha *et al.*, 2024a] Yaohua Zha, Huizhen Ji, Jinmin Li, Rongsheng Li, Tao Dai, Bin Chen, Zhi Wang, and Shu-Tao Xia. Towards compact 3d representations via point feature enhancement masked autoencoders. In *Proceedings of the AAAI Conference on Artificial Intelligence*, volume 38, pages 6962–6970, 2024. 1, 2, 5, 7
- [Zha *et al.*, 2024b] Yaohua Zha, Naiqi Li, Yanzi Wang, Tao Dai, Hang Guo, Bin Chen, Zhi Wang, Zhihao Ouyang, and Shu-Tao Xia. Lcm: Locally constrained compact point cloud model for masked point modeling. *arXiv preprint arXiv:2405.17149*, 2024. 2
- [Zhang *et al.*, 2021] Zaiwei Zhang, Rohit Girdhar, Armand Joulin, and Ishan Misra. Self-supervised pretraining of 3d features on any point-cloud. In *Proceedings of the IEEE/CVF International Conference on Computer Vision (ICCV)*, pages 10252–10263, October 2021. 6
- [Zhang *et al.*, 2022a] Renrui Zhang, Ziyu Guo, Peng Gao, Rongyao Fang, Bin Zhao, Dong Wang, Yu Qiao, and Hongsheng Li. Point-m2ae: Multi-scale masked autoencoders for hierarchical point cloud pre-training. *arXiv preprint arXiv:2205.14401*, 2022. 5, 6, 7
- [Zhang *et al.*, 2022b] Renrui Zhang, Liuhui Wang, Yu Qiao, Peng Gao, and Hongsheng Li. Learning 3d representations from 2d pre-trained models via image-to-point masked autoencoders. *arXiv preprint arXiv:2212.06785*, 2022. 5, 6, 7
- [Zhou *et al.*, 2024] Xin Zhou, Ding kang Liang, Wei Xu, Xingkui Zhu, Yihan Xu, Zhikang Zou, and Xiang Bai. Dynamic adapter meets prompt tuning: Parameter-efficient transfer learning for point cloud analysis. In *Proceedings of the IEEE/CVF Conference on Computer Vision and Pattern Recognition*, pages 14707–14717, 2024. 3